Journal of Alloys and Compounds 489 (2010) L13–L16

Contents lists available at ScienceDirect

Journal of Alloys and Compounds

journal homepage: www.elsevier.com/locate/jallcom

Letter

Effect of H_2/CO_2 mixture gas treatment temperature on the activity of $LaNiO_3$ catalyst for hydrogen production from formaldehyde aqueous solution under visible light

Lishan Jia*, Juanjuan Li, Weiping Fang

Department of Chemical Engineering and Biochemical Engineering and Department of Chemistry, College of Chemistry and Chemical Engineering, Xiamen University, Xiamen 361005, Fujian, China

ARTICLE INFO

Article history:
Received 29 June 2009
Received in revised form
15 September 2009
Accepted 15 September 2009
Available online 25 September 2009

Keywords:
Visible light
Hydrogen
$Ni/LaNiO_{3-\delta}–La_2O_2CO_3$
Photocatalyst
H_2/CO_2 mixture gas

ABSTRACT

H_2/CO_2 mixture gas treatment at moderate temperature is found to be effective in improving the activity of $LaNiO_3$ catalyst for hydrogen production from formaldehyde aqueous solution under visible light. The $LaNiO_3$, as a precursor, was treated at various temperatures (573–973 K) for 4 h under continuous flow mixture gas with a molar ratio of H_2/CO_2 = 4:1. Among all the resultant photocatalyst, the $LaNiO_3$ treated at 773 K ($Ni/LaNiO_{3-\delta}–La_2O_2CO_3$), exhibited highest photocatalytic activity when exposed to visible-light irradiation and was further characterized by XRD, SEM, TEM, UV-diffuse reflectance spectroscopy. The results indicated that $Ni/LaNiO_{3-\delta}–La_2O_2CO_3$ photocatalyst had narrow bandgap and can efficiently transfer photogenerated electrons on the surface and thus reduce H^+ to hydrogen.

1. Introduction

Hydrogen, an attractive clean and renewable energy source, is considered as an ideal fuel for the future. Our current energy infrastructure is dominated by fossil fuel use, which leads to greenhouse gas emissions. If we can synthesize a catalyst to produce hydrogen from water by harvesting sunlight, it could be a key to solve these problems. However, most of developed photocatalysts capable of splitting water can work only in the ultraviolet region [1–7]. To effectively utilize the visible light that accounts for 43% of the solar spectrum [8], it is therefore necessary to develop a visible-light responsive photocatalyst, and substantial efforts have been made in recent years to explore such a material. The photocatalytic activity can be enhanced by loading metal oxide and/or metal on various semiconductors as cocatalyst [9–11]. For example, Wu et al. [12] reported that NiO–Ni–$InTaO_4$ prepared by an innovative sol–gel method exhibited high photocatalytic activity for water splitting under visible-light irradiation. Domen research group [13] synthesized Rh/Cr_2O_3-loaded $(Ga_{1-x}Zn_x)(N_{1-x}O_x)$ catalyst with high catalytic activity for overall water splitting under visible-light irradiation, and found that both Rh and Cr_2O_3 are indispensable for achieving photocatalytic overall water splitting in this $(Ga_{1-x}Zn_x)(N_{1-x}O_x)$-based system.

As reported previously [14], the $LaNiO_3$ could be rapidly modified at moderate temperature under a stoichiometric mixture of CH_4 and CO_2. The resultant $Ni–La_2O_2CO_3$ catalyst showed high activity and stability for the CO_2 reforming of methane reaction, which can be attributed to the high dispersion of metal Ni. Based on the above reports, we think whether it is possible to synthesize a catalyst containing metallic nickel, nickel oxide and oxycarbonate species. Therefore, the $LaNiO_3$, as a precursor, was treated at various temperatures for 4 h under continuous flow mixture gas with a molar ratio of H_2/CO_2 = 4:1. In the present work, the effect of H_2/CO_2 mixture gas treatment temperature on the activity of $LaNiO_3$ for hydrogen production from formaldehyde aqueous solution under visible light is investigated by characterization analysis.

2. Experimental

2.1. Catalyst synthesis

The precursor $LaNiO_3$ was prepared by sol–gel method [15]. $La(NO_3)_3{\cdot}nH_2O$ and $Ni(NO_3)_3{\cdot}6H_2O$ were weighed in equimolar amounts and dissolved in distilled water, then citric acid was added into the mixed solution under vigorous stirring with a citric acid/total cations molar ratio of 1/2. The excess water was slowly removed under infrared lamp irradiation until a viscous liquid was produced. Subsequently, the prolonged heating formed a crispy and bubbly precursor with black colour [16]. The obtained samples were manually ground with an agate mortar, and then they were calcined at 673 K for 2 h, and at 1073 K for 4 h to form $LaNiO_3$ perovskite phase.

450 mg of the $LaNiO_3$ powder was packed into the reactor and heated to the specified temperature (573–973 K) at a rate of 283 K min^{-1}, and then maintained at

* Corresponding author. Tel.: +86 592 2188283; fax: +86 592 2184822.
E-mail address: Jials@xmu.edu.cn (L. Jia).

0925-8388/$ – see front matter © 2009 Elsevier B.V. All rights reserved.
doi:10.1016/j.jallcom.2009.09.104

that temperature for 4 h in a flow of H_2/CO_2 mixture (20 ml min^{-1}). After that, the sample was cooled to room temperature under mixture flow.

2.2. Catalyst characterization

X-ray diffraction (XRD) patterns were obtained on a Panalytical X-pert spathic powder diffractometer with Cu-Ka radiation source. The accelerating voltage and the applied current were 40 kV and 30 mA, respectively.

Hydrogen-temperature-programmed reduction (TPR) was performed with a quartz tube fixed-bed micro-reactor. Prior to the TPR measurement, each 50 mg catalyst sample was pretreated in Argon at 573 K for 30 min. After being cooled to 303 K, the sample was exposed to flow (30 ml min^{-1}) of 5 vol.% H_2/Ar and ramped to 933 K at a heating rate of 283 K min^{-1}.

SEM images of the samples were obtained on a LEO1530 scanning electron microscope. Transmission electron microscopy (TEM) was performed on a Phillips Analytical FEI Tecnai 30 electron microscope operated at an acceleration voltage of 300 kV.

Ultraviolet–visible (UV–vis) diffuse reflection spectroscopy of the photocatalysts was recorded using a Varian Cary 5000 UV–vis spectrophotometer. The spectra were collected in the 200–800 nm range at room temperature using $BaSO_4$ as a reference.

2.3. Photocatalytic splitting of water

The photocatalytic reaction was evaluated in a self-made quartz inner irradiation type reaction vessel. The catalyst (0.1 g) was suspended in aqueous formaldehyde solution (H_2O 175 mL, HCHO 25 mL) by a magnetic stirrer. Prior to irradiation, the solution was continuously bubbled with N_2 at a rate of 60 ml min^{-1} for 30 min, and then the gas content was checked by GC to confirm that no oxygen was present. 2 mol/L $NaNO_2$ solution introduced into the water jacket as an internal circulation cooling medium to eliminate UV-light (cut-off $\lambda < 400$ nm) [17,18]. Irradiation was conducted using a 125 W xenon lamp and the reaction temperature was kept at 323 K.

The gas evolved was gathered and analysed by GC (TCD, molecular sieve 5 Å column and Ar carrier). Blank reactions were carried out without catalyst under visible-light irradiation and no production of hydrogen was observed.

3. Results and discussion

3.1. XRD analysis

Fig. 1 shows the powder X-ray diffraction (XRD) patterns of samples with different treatment temperatures, along with $LaNiO_3$ data for comparison. The X-ray diffraction analysis exhibits that at 573 K, the structure of perovskite is preserved and the main phase detected was $LaNiO_{2.7}$; at 673 K, the predominant phases are $LaNiO_{2.7}$ and nickel oxide; it begins to change at around 773 K; at this temperature, the main phase detected was lanthanum oxycarbonate $La_2O_2CO_3$ (JCPDS 01-084-1963). This is because the $LaNiO_3$ treated at 773 K under H_2/CO_2 mixture gas, was reduced into La_2O_3 and La_2O_3 further reacted with CO_2 to form $La_2O_2CO_3$. Diffractive peaks indexed to metal Ni can also be found at $2\theta = 44.349^\circ$, indicating that the Ni ions are effectively reduced into metal Ni. Besides, there was a slight indication of the formation of the $LaNiO_{2.7}$ phase with a line at $2\theta = 32.828^\circ$ and 67.9288°. At 873 and 973 K, $LaNiO_3$ was completely destroyed, the only phases detected being $La_2O_2CO_3$ and metallic nickel Ni. The sample obtained at 773 K was designated as Ni/$LaNiO_{3-\delta}$–$La_2O_2CO_3$. The details of samples are summarized in Table 1.

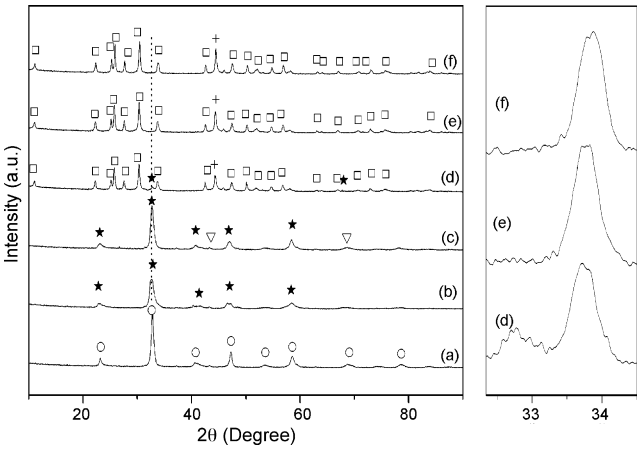

Fig. 1. XRD analysis of (a) $LaNiO_3$ before treatment and after treatment at various temperatures: (b) 573 K; (c) 673 K; (d) 773 K; (e) 873 K; (f) 973 K. (◯) $LaNiO_3$, (⋆) $LaNiO_{2.7}$, (▽) NiO, (+) Ni and (□) $La_2O_2CO_3$.

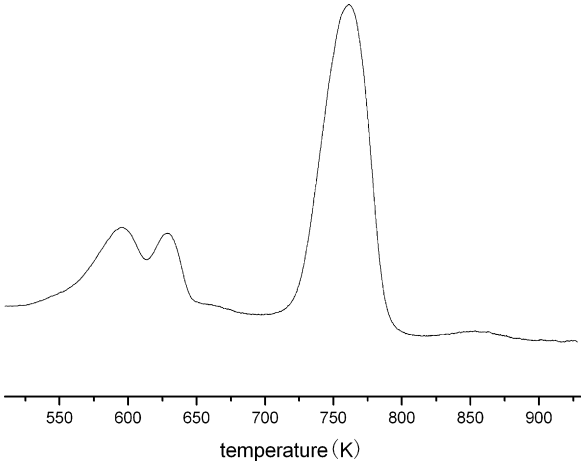

Fig. 2. TPR curves of the $LaNiO_3$. Weight: 50 mg; gas flow rate: 5% H_2/Ar, 30 ml min^{-1}.

3.2. TPR analysis

Analysis of the reduction profiles of $LaNiO_3$ (Fig. 2) shows two peak formations, which correspond to different Ni intermediate species. We can observe that the first reduction event takes place at low temperatures between 513 and 653 K. This peak was split into two peaks, one at 594 K and the other at 627 K, which is probably due to the similar reduction properties of Ni^{3+} and Ni^{2+} in the $LaNiO_3$ matrix. The first peak at 594 K corresponds to the formation of the $LaNiO_{2.7}$ without total destruction of the perovskite-type structure, tolerating a significant oxygen deficiency phase, and the second peak at 627 K is due to the partially reduction of Ni^{3+} to Ni^{2+}. The highest temperature peak appears centred at around 761 K, corresponding to Ni^0 and La_2O_3. Based on these results, the reduction

Table 1
X-ray diffraction analysis and bandgap of different samples.

Main phase (calcined)	Treatment temperature (K)	Main phase (after treated)	Bandgap (eV)
$LaNiO_3$	Untreated	$LaNiO_3$	–
$LaNiO_3$	573	$LaNiO_{2.7}$	2.73
$LaNiO_3$	673	$LaNiO_{2.7}$, NiO	2.52
$LaNiO_3$	773	$La_2O_2CO_3$, $LaNiO_{2.7}$, Ni	2.42
$LaNiO_3$	873	$La_2O_2CO_3$, Ni	2.87
$LaNiO_3$	973	$La_2O_2CO_3$, Ni	2.90

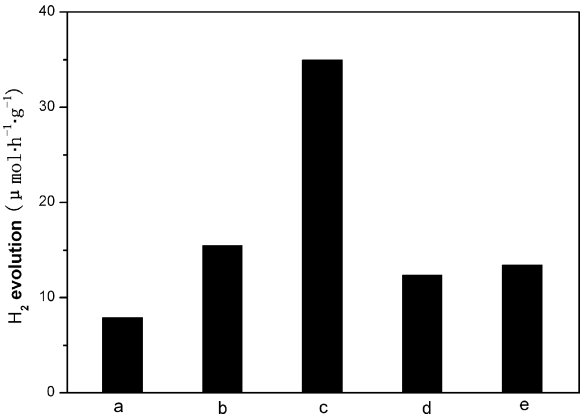

Fig. 3. Initial rates of H_2 evolution in formaldehyde aqueous solution over $LaNiO_3$ after treatment at (a) 573 K, (b) 673 K, (c) 773 K, (d) 873 K and (e) 973 K.

steps are written as follows:

$$LaNiO_3 + H_2 \rightarrow LaNiO_{2.7} + NiO + H_2 \quad \text{(between 513 and 653 K)}$$

$$LaNiO_{2.7} + H_2 \rightarrow La_2O_3 + Ni + H_2 \quad \text{(between 683 and 803 K)}$$

3.3. Effect of treatment temperature on photocatalytic activity

The photocatalytic activity of $LaNiO_3$ for hydrogen production from formaldehyde aqueous solution was negligible. However, the treatment of $LaNiO_3$ with continuous H_2/CO_2 mixture flow at different temperatures resulted in clearly observable H_2 evolution, which were shown in Fig. 3. The rates of H_2 evolution varied with treatment temperature to a maximum at 773 K with activities of 36 μmol h^{-1} g^{-1}, beyond which the activity of the sample abruptly dropped. No O_2 evolution occurs during the reaction due to the irreversible consumption of formaldehyde by photogenerated holes in the valence band of the photocatalyst [19].

3.4. SEM measurement

Fig. 4 shows SEM images of the prepared samples, along with $LaNiO_3$ data for comparison. When treated at 573–773 K, the particle became more uniform. The 773 K treated sample displays regularly shaped particles. However, treatment at 873 and 973 K showed similar feature that the grains became irregular and some aggregated together.

3.5. TEM and DRS measurement

Fig. 5(a) displays the TEM images of the $LaNiO_3$ treated at 773 K. There are some dotted dark spots less than 9 nm, which should be the reduced Ni species and some light small crystals that was possibly the $LaNiO_{3-\delta}$ species. The Ni and $LaNiO_{3-\delta}$ particles are highly dispersed in the $La_2O_2CO_3$, which made it possible for the reactant easily gets in contact with the catalytic active site [20].

The bandgap for the Ni/$LaNiO_{3-\delta}$–$La_2O_2CO_3$ is evaluated by the extrapolation method, which is shown in Fig. 5(b). The positions of the bandgap were determined by the interception of the straight line fitted through the low-energy side of the curve $[F(R_\infty)\cdot h\nu]^2$ versus $h\nu$, where $F(R_\infty)$ is the Kubelka–Munk function and $h\nu$ is the energy of the incident photon [21,22]. The sample shows a bandgap-narrowing at roughly 2.42 eV, which can effectively absorb visible light. However, the sample $LaNiO_3$ calcined at 1073 K showed no bandgap, indicating the rhombohedral $LaNiO_3$ does not display any optical absorption [23]. The energy values of different samples are summarized in Table 1.

3.6. Stability of photocatalytic activity on Ni/$LaNiO_{3-\delta}$–$La_2O_2CO_3$

Fig. 6 shows the time course of H_2 evolution from an aqueous formaldehyde solution under visible light ($\lambda > 420$ nm) using

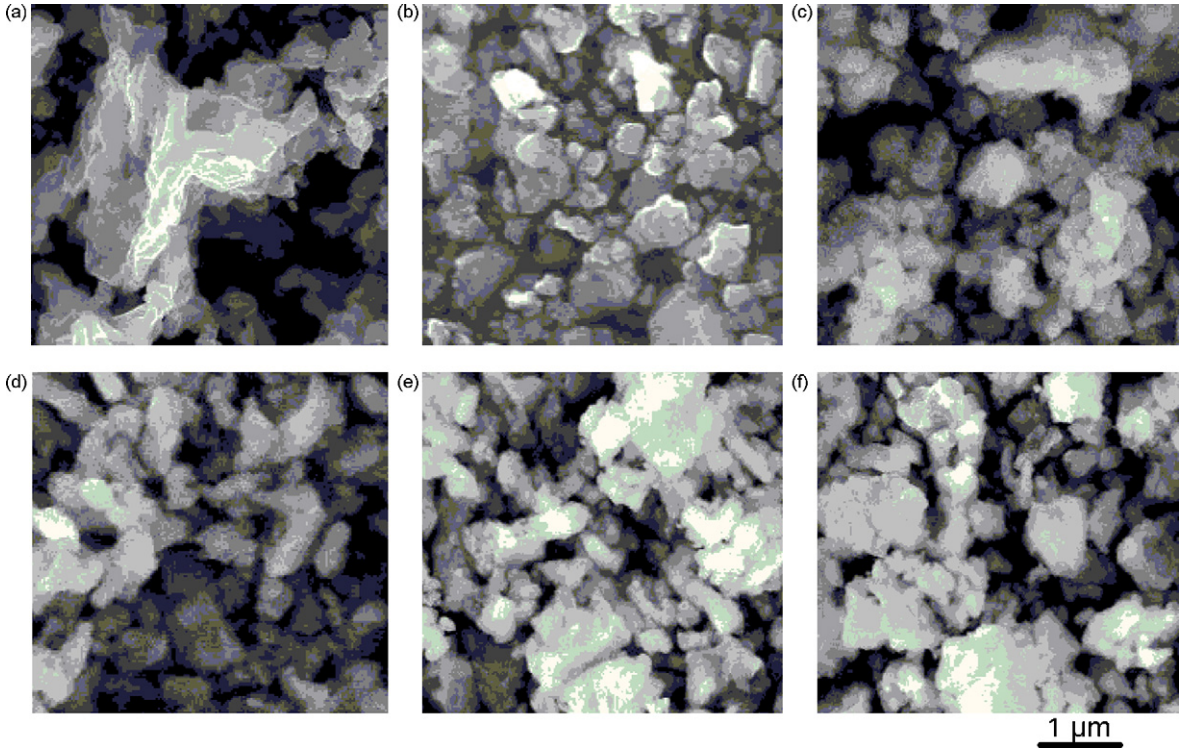

Fig. 4. SEM images of (a) $LaNiO_3$, (b–f) $LaNiO_3$ samples treated at (b) 573 K, (c) 673 K, (d) 773 K (e) 873 K and (f) 973 K.

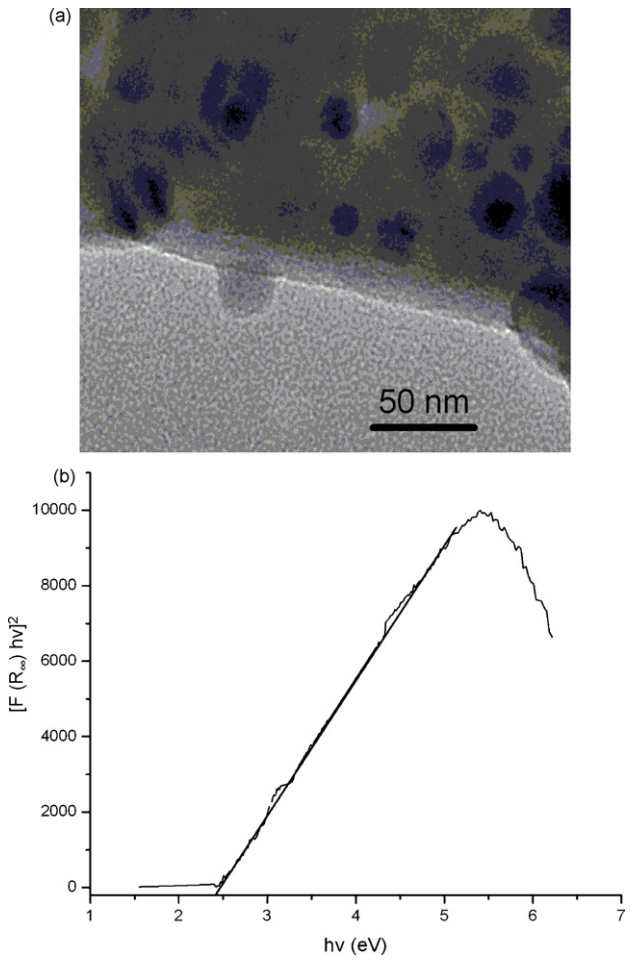

Fig. 5. (a) TEM images of $LaNiO_3$ treated at 773 K ($Ni/LaNiO_{2.7}$–$La_2O_2CO_3$). (b) Transformed diffuse reflectance spectra of $Ni/LaNiO_{2.7}$–$La_2O_2CO_3$.

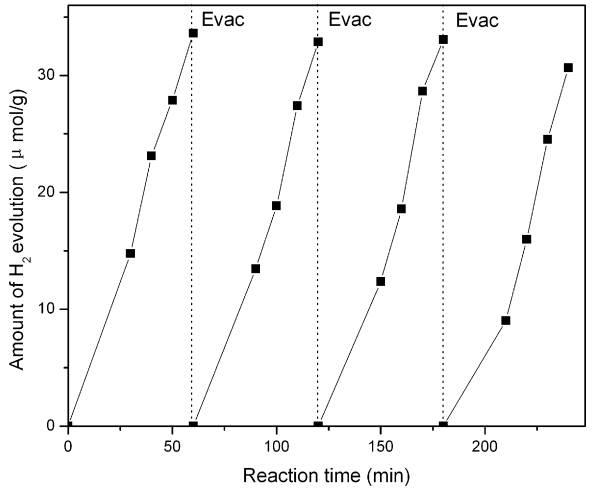

Fig. 6. Time courses of hydrogen production from formaldehyde aqueous solution under visible irradiation on sample $Ni/LaNiO_{3-\delta}$–$La_2O_2CO_3$.

sample $Ni/LaNiO_{3-\delta}$–$La_2O_2CO_3$. The rate of H_2 evolution in the second and subsequent runs with intermittent evacuation was also unchanged, and the reaction continued to proceed steadily. The experimental results demonstrate that the catalyst has a good reproducibility and can be used repeatedly. Therefore, $Ni/LaNiO_{3-\delta}$–$La_2O_2CO_3$ is a stable catalyst for photocatalytic H_2 evolution under visible-light irradiation.

4. Conclusions

The catalytic activity for overall water splitting under visible light was found to be improved by $LaNiO_3$ treated at moderate temperature under a flow of H_2/CO_2 mixture. The degree of activity improvement was dependent on the treatment temperature. The results showed that $LaNiO_3$ treated at 773 K, had the highest photocatalytic activity for overall water splitting. XRD measurements revealed that the sample prepared at 773 K contains a mixture of $LaNiO_{2.7}$ and metallic nickel Ni and $La_2O_2CO_3$. The optical absorption edge of sample shifted to the low-energy region, as proven in DRS. TEM results showed that Ni and $LaNiO_{2.7}$ particles dispersed on $La_2O_2CO_3$ as a cocatalyst. All these indicated the catalyst should be an active photocatalyst under visible-light irradiation.

Acknowledgments

This work was supported by the Key Laboratory for Chemical Biology of Fujian Province and State Key Laboratory for Physical Chemistry of Solid Surface of Xiamen University. We thank the Analysis and Testing Centre of Xiamen University for the analysis and observation work.

References

[1] H.Y. Lin, H.C. Huang, W.L. Wang, Micropor. Mesopor. Mater. 115 (2008) 568–575.
[2] M.C. Sarahan, E.C. Carroll, M. Allen, D.S. Larsen, N.D. Browning, F.E. Osterloh, J. Solid State Chem. 181 (2008) 1678–1683.
[3] K. Shimizu, S. Itoh, T. Hatamachi, T. Kodama, M. Sato, K. Toda, Chem. Mater. 17 (2005) 5161–5166.
[4] Y. Ebina, N. Sakai, T. Sasaki, J. Phys. Chem. B 109 (2005) 17212–17216.
[5] A. Kudo, H. Kato, S. Nakagawa, J. Phys. Chem. B 104 (2000) 571–575.
[6] O.C. Compton, C.H. Mullet, S. Chiang, F.E. Osterloh, J. Phys. Chem. C 112 (2008) 6202–6208.
[7] J. Yin, Z. Zou, J.H. Ye, J. Phys. Chem. B 108 (2004) 12790–12794.
[8] D.F. Wang, T. Kako, J.H. Ye, J. Am. Chem. Soc. 130 (2008) 2724–2725.
[9] M. Yoshida, K. Takanabe, K. Maeda, A. Ishikawa, J. Kubota, Y. Sakata, Y. Ikezawa, K. Domen, J. Phys. Chem. C 113 (2009) 10151–10157.
[10] A. Yamakata, T. Ishibashi, H. Kato, A. Kudo, H. Onishi, J. Phys. Chem. B 107 (2003) 14383–14387.
[11] J.S. Jang, D.J. Ham, N. Lakshminarasimhan, W.Y. Choi, J.S. Lee, Appl. Catal. A: Gen. 346 (2008) 149–154.
[12] Y.C. Chiou, U. Kumar, J.C.S. Wu, Appl. Catal. A: Gen. 357 (2009) 73–78.
[13] K. Maeda, K. Teramura, D.L. Lu, N. Saito, Y. Inoue, K. Domen, J. Phys. Chem. C 111 (2007) 7554–7560.
[14] C.B. Dupeyrat, G.A.S. Gallego, F. Mondragon, J. Barrault, J.M. Tatibouet, Catal. Today 107–108 (2005) 474–480.
[15] Z. Yang, Y. Huang, B. Dong, H.L. Li, J. Solid State Chem. 178 (2005) 1157–1164.
[16] M. Popa, M. Kakihana, Solid State Ionics 151 (2002) 251–257.
[17] K. Maeda, K. Teramura, K. Domen, J. Catal. 254 (2008) 198–204.
[18] C.J. Xing, Y.J. Zhang, W. Yan, L.J. Guo, Int. J. Hydrogen Energy 31 (2006) 2018–2024.
[19] A. Galińska, J. Walendziewski, Energy Fuels 19 (2005) 1143–1147.
[20] Bannat S I., K. Wessels, T. Oekermann, J. Rathousky, D. Bahnemann, M. Wark, Chem. Mater. 21 (2009) 1645–1653.
[21] H. Weiû, A. Fernandez, H. Kisch, Angew. Chem. Int. Ed. 40 (2001) 3825–3827.
[22] R.S.G. Ferreira, P.G.P. de Oliveira, F.B. Noronha, Appl. Catal. B: Environ. 29 (2001) 275–283.
[23] M. Biswas, J. Alloys Compd. 480 (2009) 942–946.